Ionized Gas

- Source of ionization & diagnostics
- HII regions
  - Sizes
  - Detection
  - Spatial Distribution
  - Connection with star formation
- Diffuse Ionized Gas
- Outflows
- Lyman alpha emission

Ionized gas: Two main mechanisms

- Shocks
  - Collisions (usually w/ e-) transfer KE to bound e-
  - If KE > ionization energy, e- is freed
- Photoionization
  - High energy (UV) photons transfer energy to bound e-
  - If $h\nu$ > ionization energy, e- is freed

Ionized gas: Other mechanisms

- Collisional ionization
  - Requires high gas densities & high temps, so not common.
  - Broad line regions of AGN
- "Compton effect" ionization
  - X-ray, γ-ray photon compton scatters, & some energy goes into ionization
- Cosmic rays
  - Can dominate ionization in dense, cold molecular cloud interiors

Shocks

- Dominate in stellar or black hole outflows (jets, winds, SNe) meeting ISM

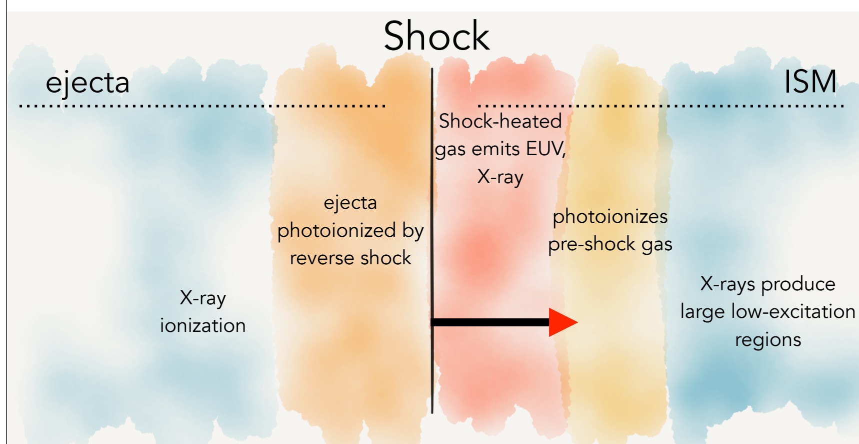

Courtesy Nell Byler

For typical ISM shocks

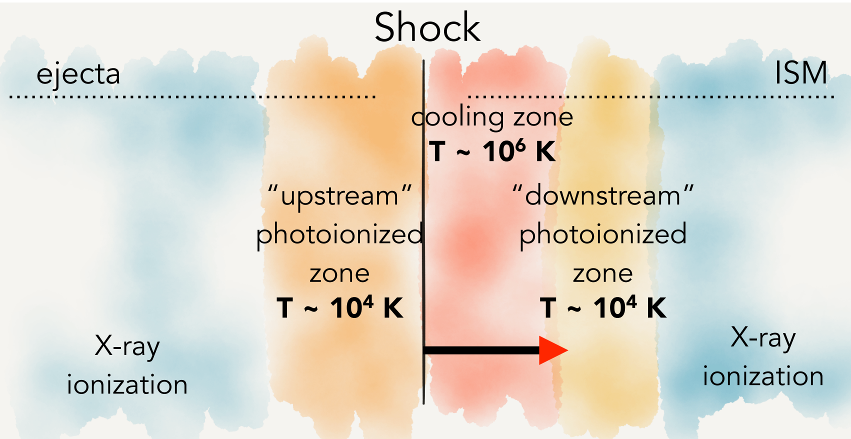

Courtesy Nell Byler

Ionization will depend on preshock T, ρ and on shock velocity

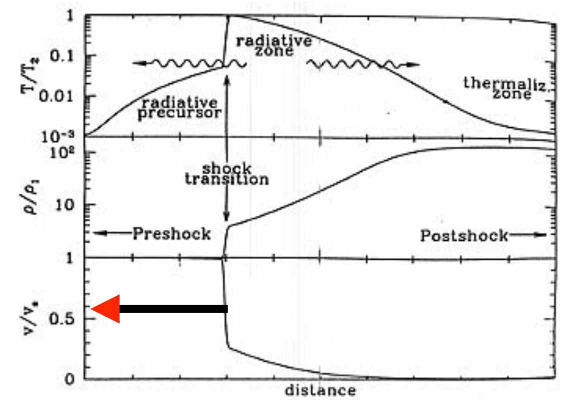

Figure 1 Schematic structure of a strong (single-fluid) shock wave showing temperature T, density ρ, and velocity v (relative to the shock front). ρ_1 is the preshock density, and T_2 is the temperature just behind the shock transition.

Draine & McKee

Photoionization

- Commonly from young O&B stars (making ionized gas a good SF tracer)
- Sometimes from hot old extreme horizontal branch (EHB) stars (LINERS?)
- Sometimes from AGN's central engine, which emits UV & X-ray photons with a roughly power-law distribution of flux ($F_\nu \propto \nu^{-\alpha}$, where $\alpha \sim 1.2\text{-}2$)

Ionized gas: Primary diagonstics

Hydrogen recombination lines

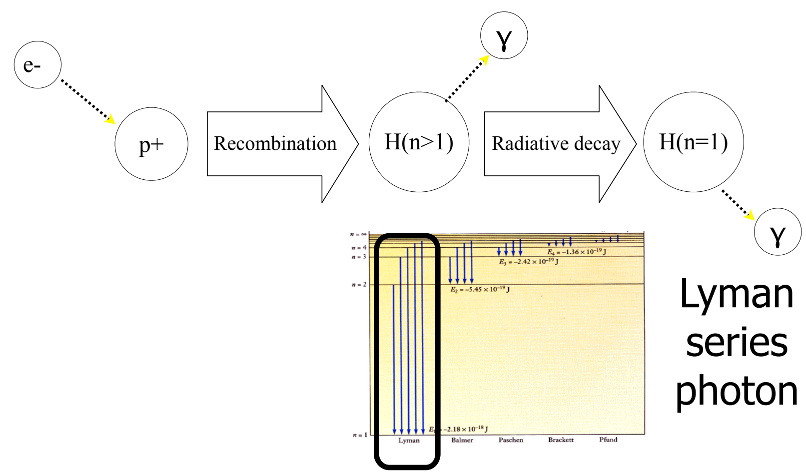

Lyman series photon

Ionized gas: Primary diagonstics

Hydrogen recombination lines

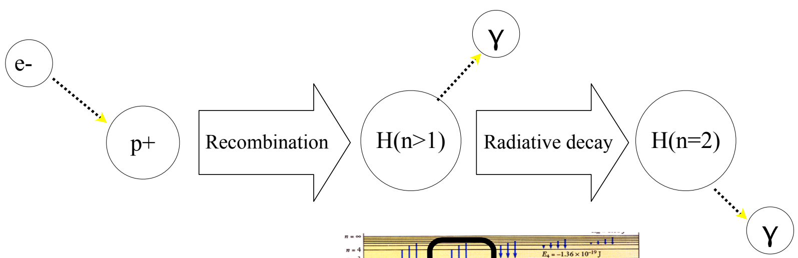

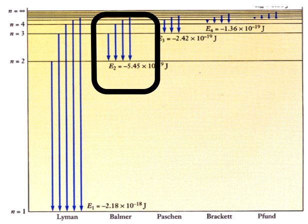

Balmer series photon

Recombination Lines of Hydrogen

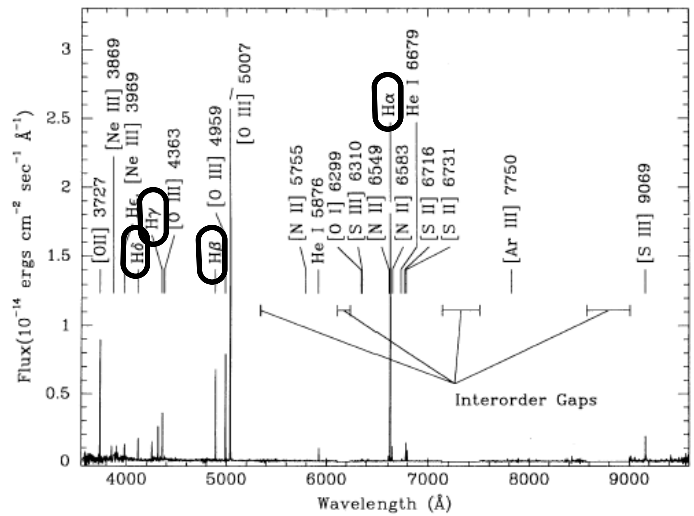

Zaritsky et al 1994

Ionized gas: Primary diagonstics

Emission lines from other ionized elements (between split energy levels in the ground state)

Excitation

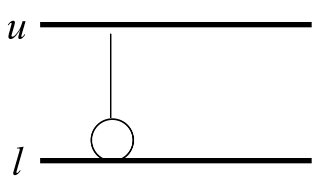

1. Collisions
2. Absorption

Decay

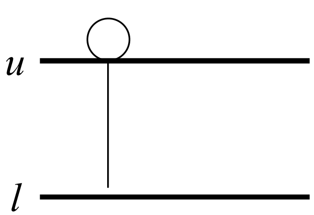

1. Collisions
2. Spontaneous Emission
3. Stimulated Emission

Emission from ionized species

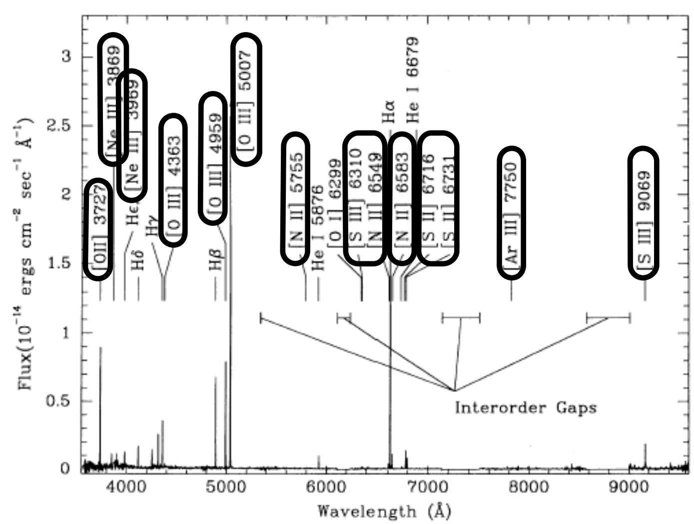

Zaritsky et al 1994

Ionized gas: Primary diagonstics

Free-free bremsstrahlung emission, and synchrotron from e- in magnetic fields (in radio)

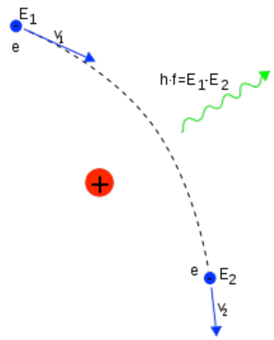

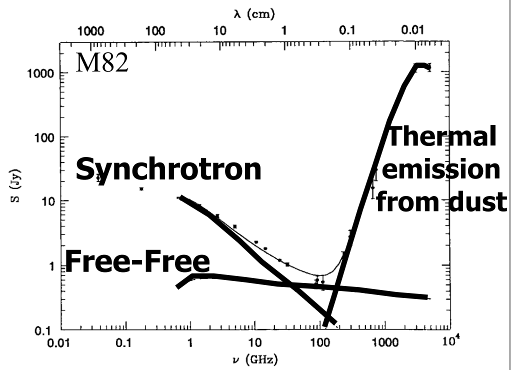

http://www.cv.nrao.edu/course/astr534/FreeFreeEmission.html
http://www.cv.nrao.edu/course/astr534/SummaryFreeFree.html
http://en.wikipedia.org/wiki/Bremsstrahlung

Photodissociation Regions

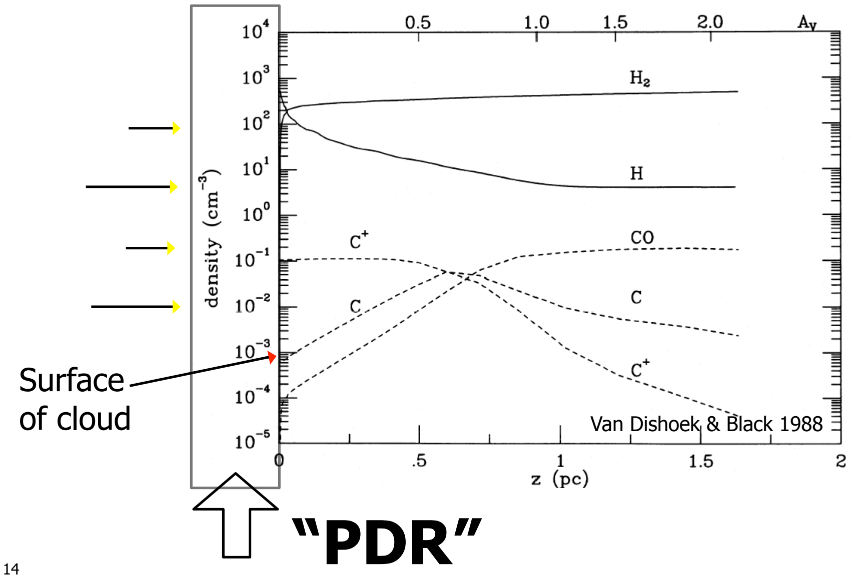

Ionized gas

Molecular Gas

Photodissociation regions (PDRs): skin of ionized gas, surrounding a skin of neutral gas, surrounding the shielded molecular gas.

The ionized gas is [redacted]ected as [redacted]n

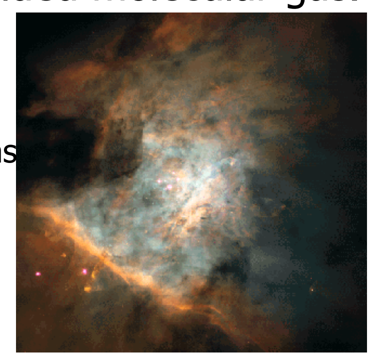

See Hollenbach & Teilens 1999 for a review of PDRs, and http://dustem.astro.umd.edu/pdrt/ for tools for interpreting PDRs

Rosette Nebula

30 Doradus: giant HII region in LMC

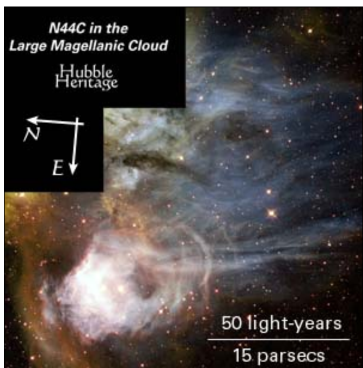

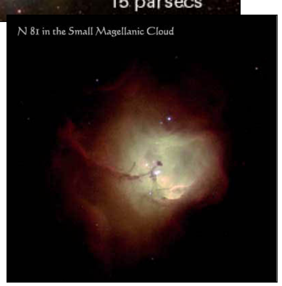

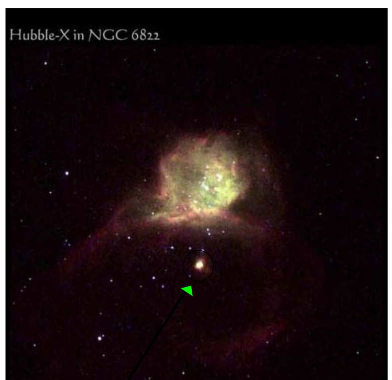

Size of Orion nebula at this distance (HII regions tend to be much bigger in low mass dwarf irregulars like NGC 6822)

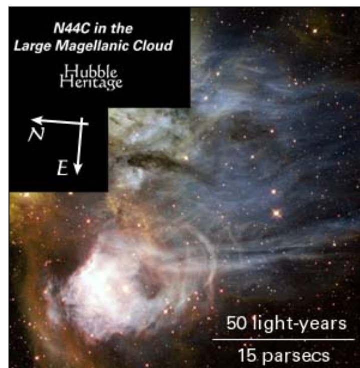

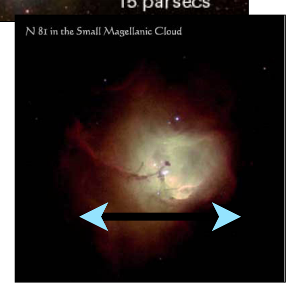

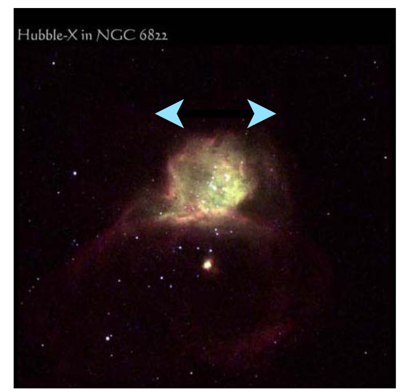

Size of HII region set by where the ionizing radiation is all used up ("Stromgren sphere")

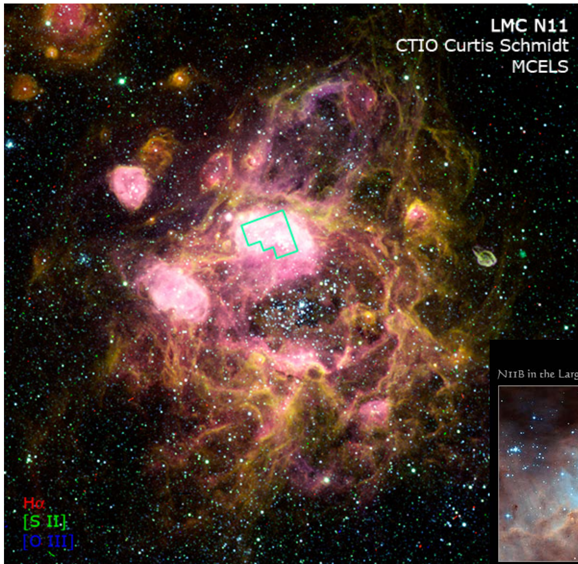

HII regions are extremely complex and are not Stromgren spheres!

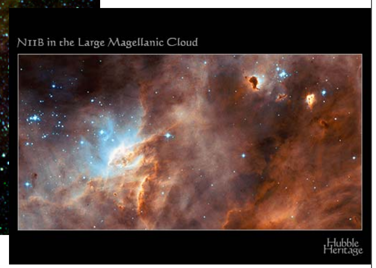

Measuring Ionized Gas: Narrow-band filters

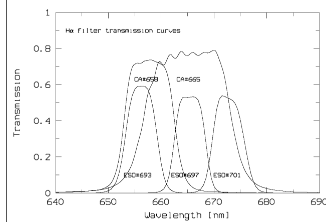

Fig. 1. Transmission curves for the ESO and Calar Alto Hα filters (ESO #693, #697, #701 and CA#658/10, CA#665/17), respectively. The plot has been generated in the MIDAS environment with the use of the implemented ESO filter and edited CAHA filter table–files.

1. Take image of galaxy through narrow filter whose wavelength covers Ha at the galaxy's redshift.
2. Take image of galaxy in "off-band".
3. Subtract to remove continuum

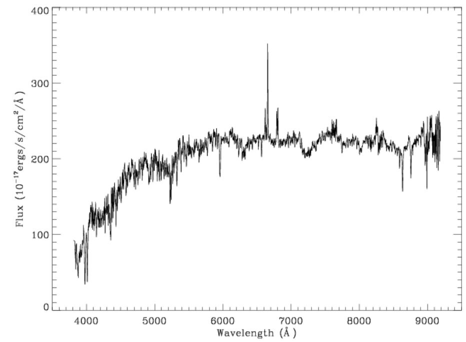

 Rossa & Dettmar 2002

HII regions cluster along spiral arms

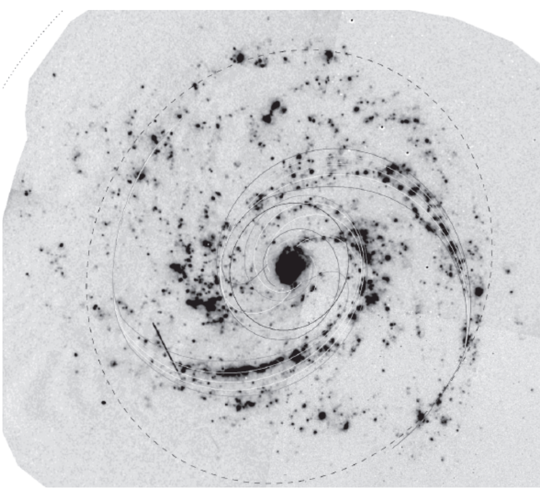

Oey et al 2003

- molecular gas forms stars
- UV from short-lived O stars photodissociate molecular gas
- gas becomes ionized in localized region
- when O stars die, gas becomes neutral

More Hα images:

Thilker et al 2002

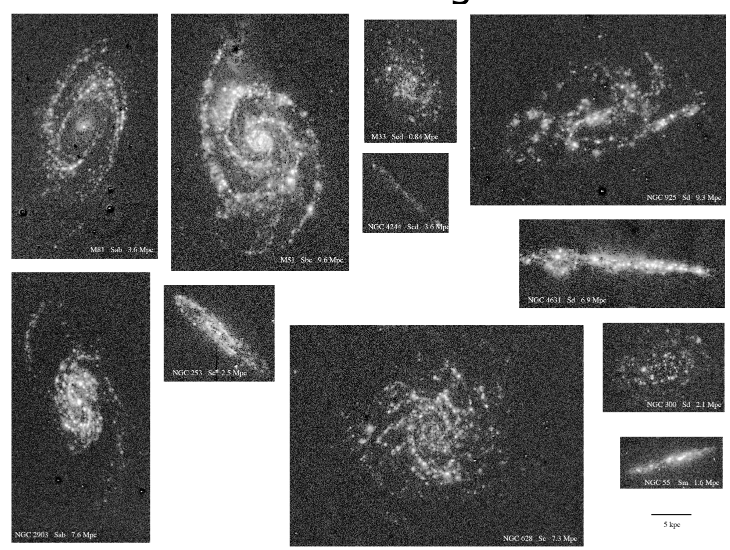

Fig. 1.—Montage of continuum-subtracted Hα images for the 10 Mpc sample. All data presented in this figure have been degraded to a common spatial resolution (100 pc), surface brightness sensitivity ($1\,\sigma = 20$ pc cm^{-6}), and pixel sampling (44 pc pixel^{-1}). Galaxies are positioned roughly according to Hubble type.

HII regions tend to have a power law distribution of luminosities

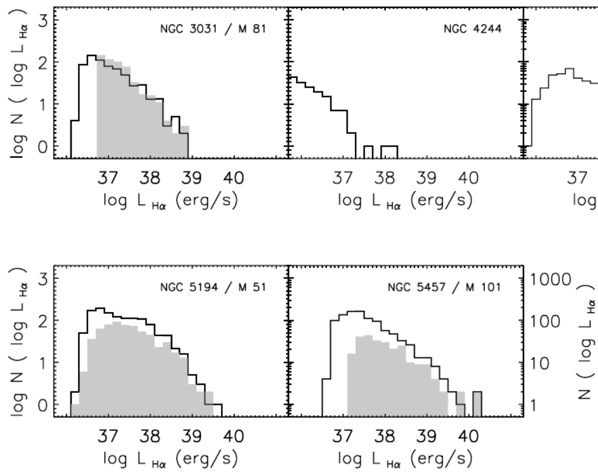

Cutoff at faint luminosities probably due to incompleteness

Thilker et al 2002

FIG. 3.—HIIphot LFs for 11 spiral galaxies viewed at full resolution and sensitivity (*solid line*), plus comparison with previous studies, when available (*shaded histogram*). References for the comparison studies are given in the text.

Most emission is in compact HII regions

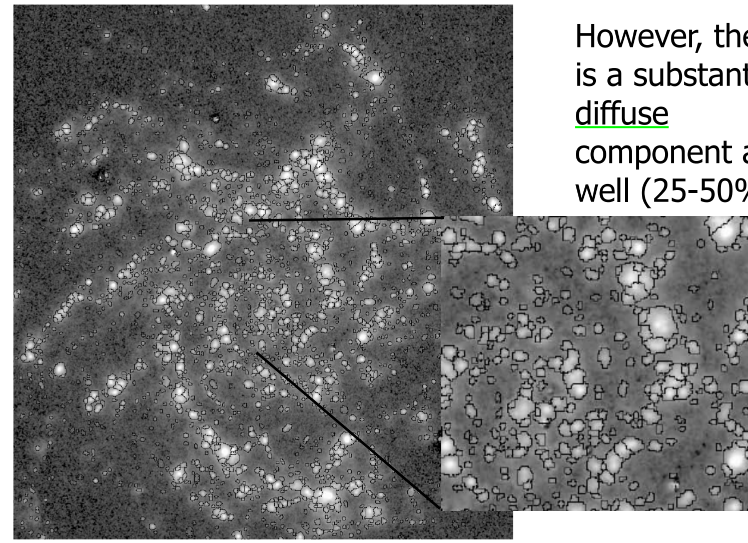

However, there is a substantial diffuse component as well (25-50%)

FIG. 2.—HIIphot boundary image for a subsection of our original resolution NGC 628 data. We have plotted boundaries based on growth to a surface brightness gradient of 1.5 EM pc^{-1} on this continuum-subtracted Hα image. Scaling is logarithmic over the interval [−5, 2000] EM.

Thilker et al 2002

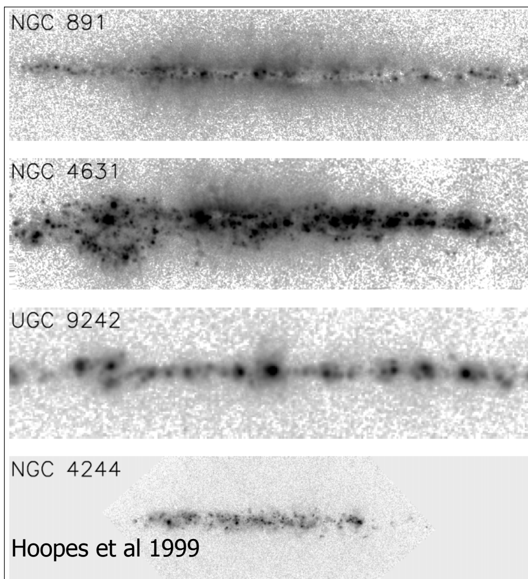

Hoopes et al 1999

The diffuse component is vertically extended ("eDIG")

Large eDIG components are associated with galaxies with high star formation rates ("leakage" from HII regions?)

FIG. 6.—Comparison of the DIG layers in the galaxies in our sample. The images have been rotated so the disk is horizontal; see Figs. 1–5 for the correct orientation. The images all have the same spatial scale, shown by the 1 kpc bar in the bottom panel. They are all displayed with the same logarithmic stretch, from −2 to 1000 pc cm^{-6}.

In extreme cases of very high star formation rates (SFRs), we can see extraplanar Hα emission from outflows

M82: a classic "starburst" gala

Red is Ha superimposed on an optical image.

Shocks & PDR!

More M82

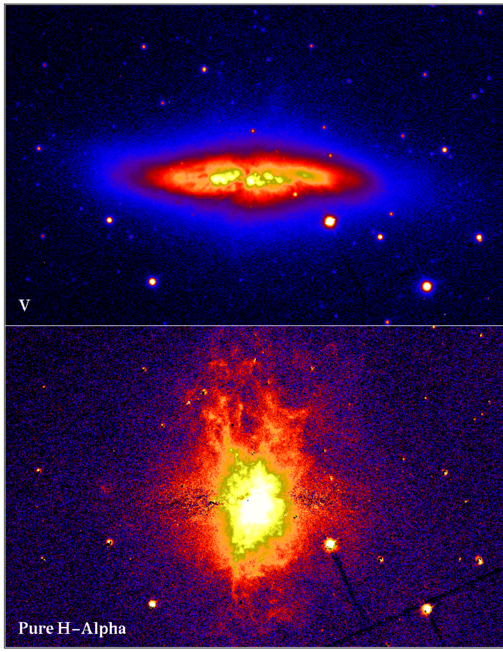

Visible

Hα

Outflow bubble in a starburst galaxy.

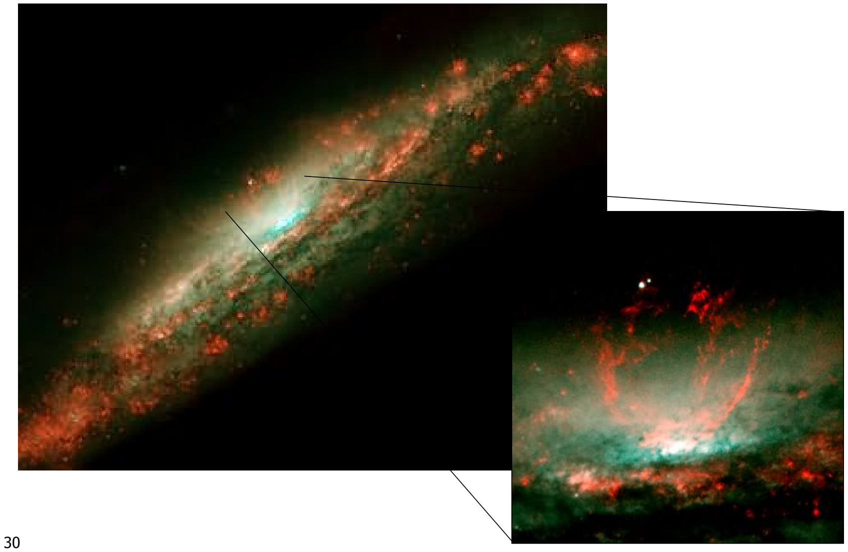

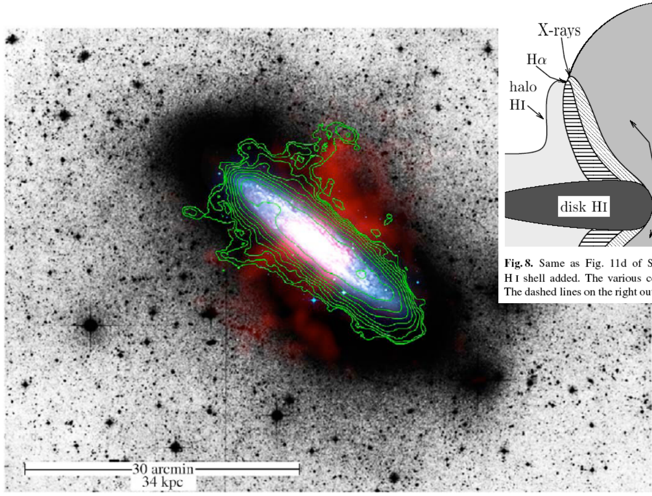

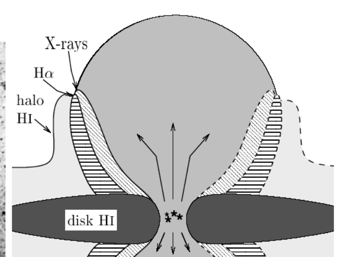

Fig. 8. Same as Fig. 11d of Strickland et al. (2002), but with an H I shell added. The various components are described in the text. The dashed lines on the right outline parts that have not been detected.

Fig. 2. Multi-wavelength image of the nearby spiral galaxy NGC 253. The deep optical image is from Malin & Hadley (1997), the blue shows the DSS optical disk, the red the X-ray emission (0.1–0.4 keV) from ROSAT (Pietsch et al. 2000), and the green contours our Compact Array H I observations. Contours are at 0.18, 0.36, 0.72, 1.4, 2.9, 5.8, 12 and 23×10^{20} cm^{-2}. The circular beam has a full half-width of 70″.

Boomsma et al 2005

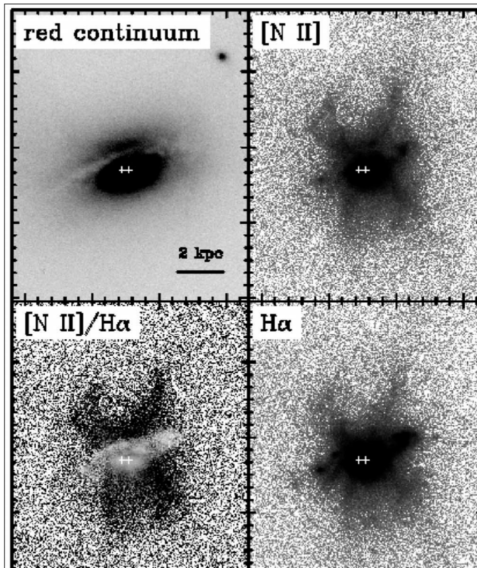

Emission lines suggestive of a strong wind (outflow). Shock heated here, though in other cases (M82), possibly photoionization heated.

Veilleux & Rupke 2002

Fig. 1.—Narrowband images of NGC 1482 obtained with the TTF. *Clockwise from upper left*: Red continuum, [N II] λ6583 line emission, Hα line emission, and [N II] λ6583/Hα ratio. Right panels are on a logarithmic intensity scale, while left panels are on a linear scale. North is at the top, and east is to the left. The positions of the continuum peaks are indicated in each image by two crosses. The spatial scale, indicated by a horizontal bar at the bottom of the red continuum image, is the same for each image and corresponds to ~21″, or 2 kpc for the adopted distance of 19.6 Mpc for NGC 1482. The [N II] λ6583/Hα ratio is below unity in the galaxy disk, but larger than unity in the hourglass-shaped nebula above and below the disk. This structure is highly suggestive of a galactic wind.

The eDIG may extend to very large scale heights when mapped at faint surface brightnesses

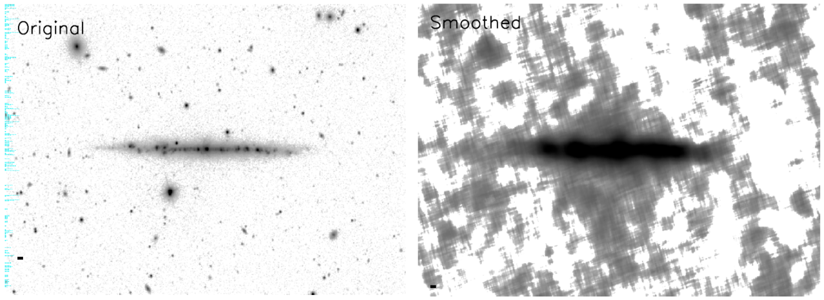

FIG. 15.—(*Lower panel*) Median filtered image of UGC 9242 compared with (*upper panel*) the original Hα + continuum image. The median box used was 207 × 20''.7. Halo emission on both sides of the disk is apparent. Scattered light from a bright star below the disk may be a problem, but no such problem exists on the north side. The upper image shows the galaxy responsible for the dark smudge in the upper left-hand corner of the image, as well as other galaxies and foreground stars that show up in the smoothed image. Features in this image are discussed in more detail in the text.

Even when there is not a massive starburst, some UV photons are escaping to ionize gas at large distances

Hoopes et al 1999

Peculiarities of the Lyman-α line

☆ "Resonance Line"

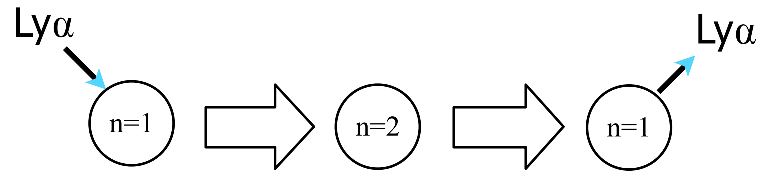

Emission line may escape galaxy at a different location than it's emitted

Peculiarities of the Lyman-α line

☆ Dust Affects Lyα emission

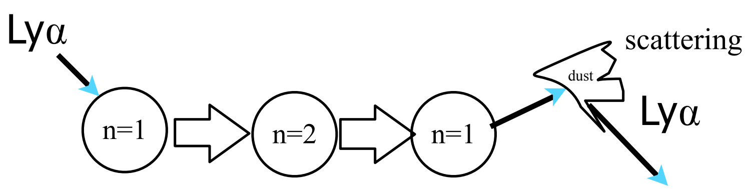

Path experiences different reddening and/or extinction than Hα or UV emission from SF region that produced original Lyα

Peculiarities of the Lyman-α line

☆ Dust Affects Lyα emission

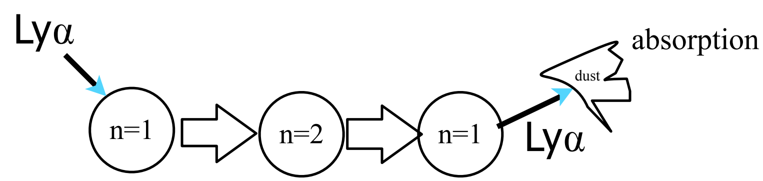

Only a small fraction of Lyα may actually escape ("escape fraction"). Longer effective path length increases chances that Lyα gets absorbed

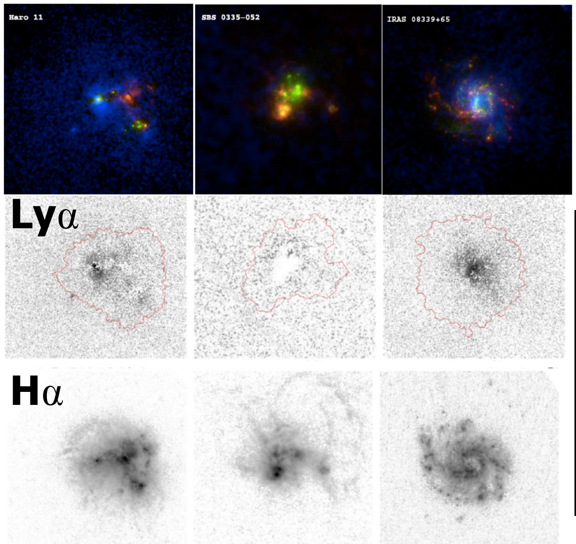

Blue: Lyα
Red: Hα

Hα and Lα don't escape from the same location

Ostlin et al 2009

Figure 1. Gray-scale images. From top to bottom: reduced F122M and F140LP; continuum subtracted Lyα resulting from unbinned images but with the $\mu_{AB,1500} = 23$ mag/□″ isophotal mask generated from binned data overlaid; adaptively filtered Lyα with F140LP isophotes overlaid; and continuum subtracted unbinned Hα. The isophotal mask from the binned data is used later for quantitative photometry. The FUV contours show 25 mag/□″ as the faintest isophote, with each subsequent isophote representing an increase by 1 mag/□″. All intensity scaling is logarithmic. North is up and east is to the left. Images are square cutouts with the length of one side in arcsec given in parentheses. From left to right: Haro 11 (20″), SBS 0335−052 (10″), and IRAS 08339+6517 (20″). In some images residual features from the ACS/SBC detector gap are visible. These areas have not been included in the photometry.

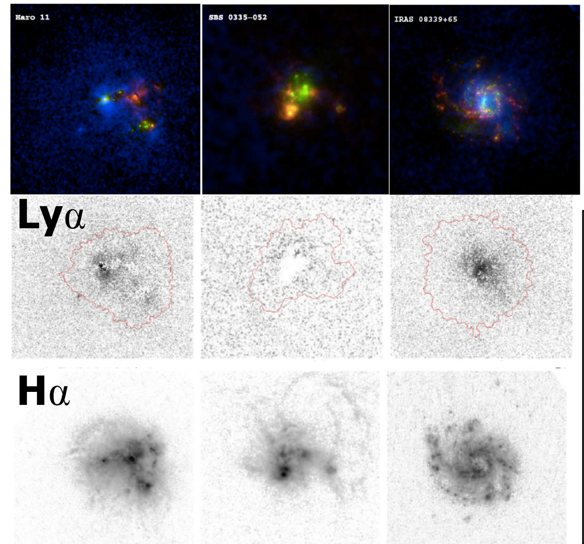

Blue: Lyα
Red: Hα

Lyα found in extended halo (resonant scattering)

Ostlin et al 2009

Figure 1. Gray-scale images. From top to bottom: reduced F122M and F140LP; continuum subtracted Lyα resulting from unbinned images but with the $\mu_{AB,1500} = 23$ mag/□″ isophotal mask generated from binned data overlaid; adaptively filtered Lyα with F140LP isophotes overlaid; and continuum subtracted unbinned Hα. The isophotal mask from the binned data is used later for quantitative photometry. The FUV contours show 25 mag/□″ as the faintest isophote, with each subsequent isophote representing an increase by 1 mag/□″. All intensity scaling is logarithmic. North is up and east is to the left. Images are square cutouts with the length of one side in arcsec given in parentheses. From left to right: Haro 11 (20″), SBS 0335−052 (10″), and IRAS 08339+6517 (20″). In some images residual features from the ACS/SBC detector gap are visible. These areas have not been included in the photometry.

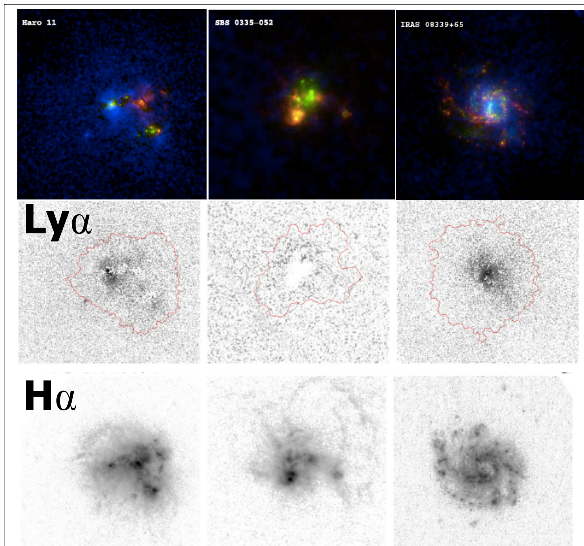

Blue: Lyα
Red: Hα

Inferred Lyα escape fractions are small (<20%)

Ostlin et al 2009

Figure 1. Gray-scale images. From top to bottom: reduced F122M and F140LP; continuum subtracted Lyα resulting from unbinned images but with the $\mu_{AB,1500} = 23$ mag/□″ isophotal mask generated from binned data overlaid; adaptively filtered Lyα with F140LP isophotes overlaid; and continuum subtracted unbinned Hα. The isophotal mask from the binned data is used later for quantitative photometry. The FUV contours show 25 mag/□″ as the faintest isophote, with each subsequent isophote representing an increase by 1 mag/□″. All intensity scaling is logarithmic. North is up and east is to the left. Images are square cutouts with the length of one side in arcsec given in parentheses. From left to right: Haro 11 (20″), SBS 0335−052 (10″), and IRAS 08339+6517 (20″). In some images residual features from the ACS/SBC detector gap are visible. These areas have not been included in the photometry.

Lyα at high redshift

1216A line moves into the optical at high-z

Used to detect galaxies and/or estimate SFR

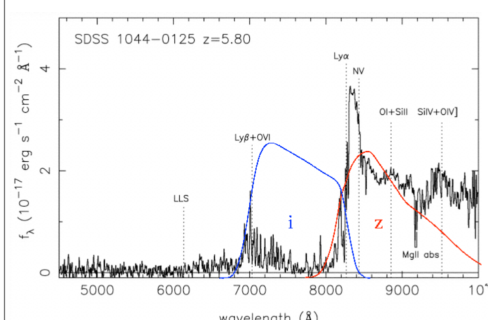

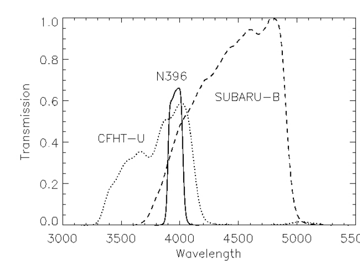

Lyα at high redshift

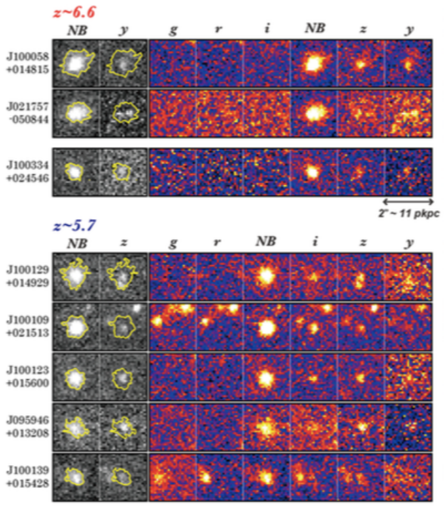

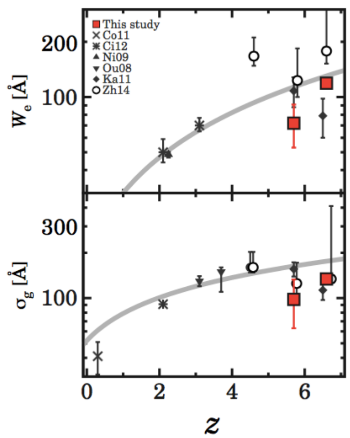

Hyper Suprime Cam: Shibuya et al 2017

Lyα at high-z

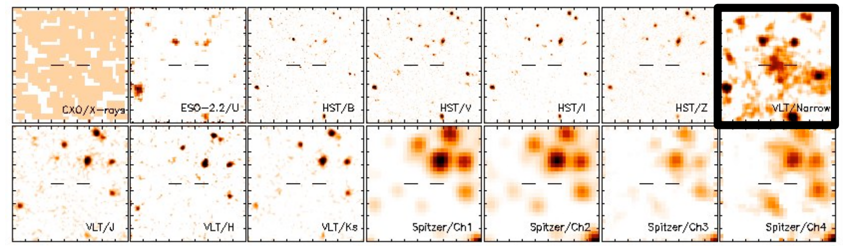

Note: Not the same galaxy. Composite below is for a slightly higher redshift

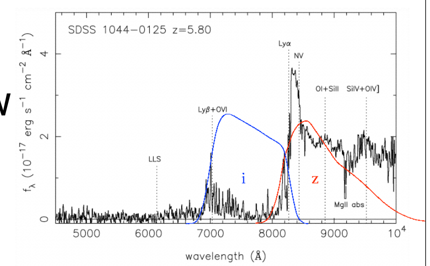

Lyα at high-z: Lyman alpha blobs

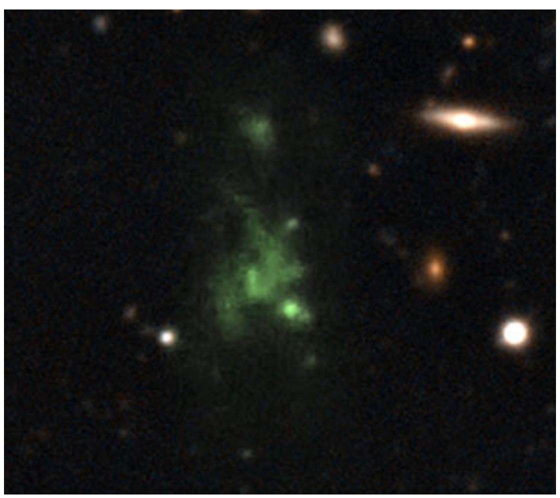

>100 kpc across

“LAB-1”: Steidel et al 2000, Matsuda et al 2000

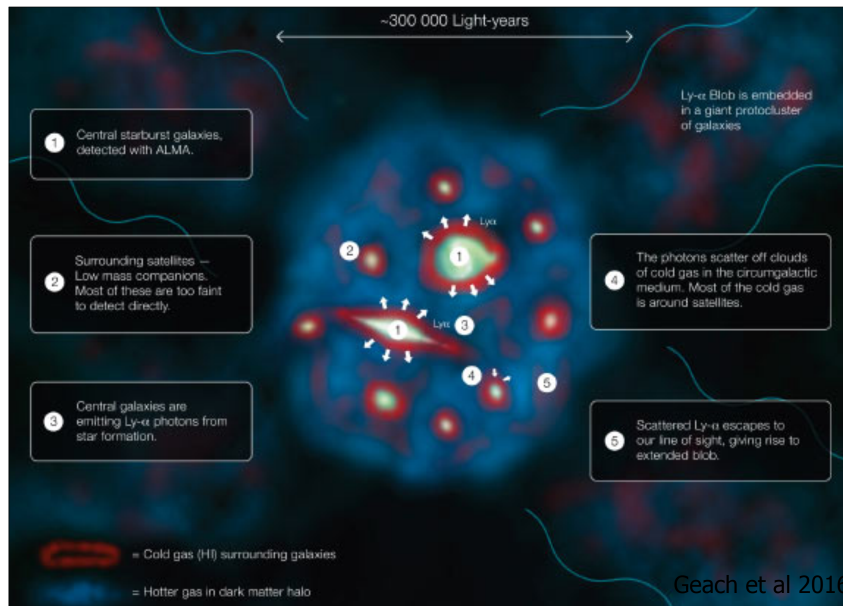

Detected AGN/galaxies interior w/ ALMA